OPEN ACCESS
Journal of Multidisciplinary Applied Natural Science Vol. xx No. xx (xxxx) https://doi.org/10.47352/jmans.2774-3047.376
Check for updates
Research Article

Evaluating the Potential of Agarose Hydrogel Incorporating Eggshell Powder as a Sustainable Medium for Seedling Growth

Ade Yeti Nuryantini*, Ea Cahya Septia Mahen, Indri Oktaviani, Bebeh Wahid Nuryadin, Dhewa Edikresnha, and Khairurrijal Khairurrijal

Received : August 13, 2025	Revised : January 5, 2026	Accepted : February 21, 2026	Online : March 20, 2026

Abstract
Hydrogels represent a promising alternative for plant cultivation, offering excellent water and nutrient retention. This study reports the synthesis and characterization of an agarose-based hydrogel composite enhanced with eggshell powder (ESP). The hydrogel composites were prepared in four agarose-to-ESP ratios: 10:0 (Hyd-ES0), 10:1 (Hyd-ES1), 10:3 (Hyd-ES3), and 10:5 (Hyd-ES5). Fourier-transform infrared spectroscopy (FTIR) analysis revealed minimal peak shifts, indicating no significant chemical modifications. Characteristic ESP peaks were identified in the composite hydrogels, confirming the effective integration of ESP into the agarose matrix. The addition of ESP reduced the decomposition rate of the hydrogels and increased macromolecular stability. Density measurements indicated higher density with increasing ESP concentration, supported by enhanced crystal formation, as evidenced by more intense diffraction peaks in X-ray diffraction (XRD) patterns. Morphological analysis revealed that the porosity of the hydrogel, swelling, and weight-loss tests showed a decline in both properties with higher ESP content. Seed germination experiments demonstrated that stem, root, and leaf growth, as well as fresh and dry weights, were most optimal with the Hyd-ES1 hydrogel composite. Thus, Hyd-ES1 hydrogel exhibits significant potential as a medium for seed germination and plant growth.

Keywords: agarose, eggshell powders, hydrogel, seedling growth

1. INTRODUCTION

Chicken eggs play a vital role in the global diet, providing an affordable and nutrient-rich food source essential for daily nutrition [1]. However, when eggs are utilized for culinary or other purposes, they inevitably leave behind eggshell waste. Eggshells represent approximately 10% of the total egg weight. Chicken eggs are produced in vast quantities each year, with a significant proportion (30%) undergoing processing within the food industry, leading to a substantial increase in eggshell waste. Eggshell waste contains abundant bioactive compounds, driving growing research efforts to develop value-added products with potential commercial applications [2]. Eggshell waste has been investigated and can be utilized in various applications, including in agriculture, the pharmaceutical industry, animal husbandry, and human nutrition. One of the eggshell applications in agriculture is plant fertilizer. Studies have demonstrated that eggshell powder can be an effective calcium supplement for plants like tomatoes and berries, helping to prevent blossom-end rot [3] as the deficiency in calcium in tomato plants leads to blossom-end rot (BER) [4]. Hence, incorporating eggshell powder into fertilizers can effectively address calcium deficiency issues.

In urban areas, direct soil-based planting is severely constrained due to limited space. As a result, methods have been developed for soilless farming. Soilless farming involves growing plants using perlite, vermiculite, sand, or hydroponics as a substitute for traditional soil. Hydroponics is the most commonly employed technique in soilless agricultural systems [5]. In hydroponic systems, the nutrient solution must be periodically refreshed to ensure stable conditions for optimal plant growth [6]. However, this operation has demonstrated limitations in some cases. For instance, frequent changes in the nutrient solution can disrupt plant growth or lead to root rot due to oxygen deficiency [7][8]. Furthermore, hydroponics requires more water than soil-based cultivation, which can be challenging in water-scarce regions. One effective

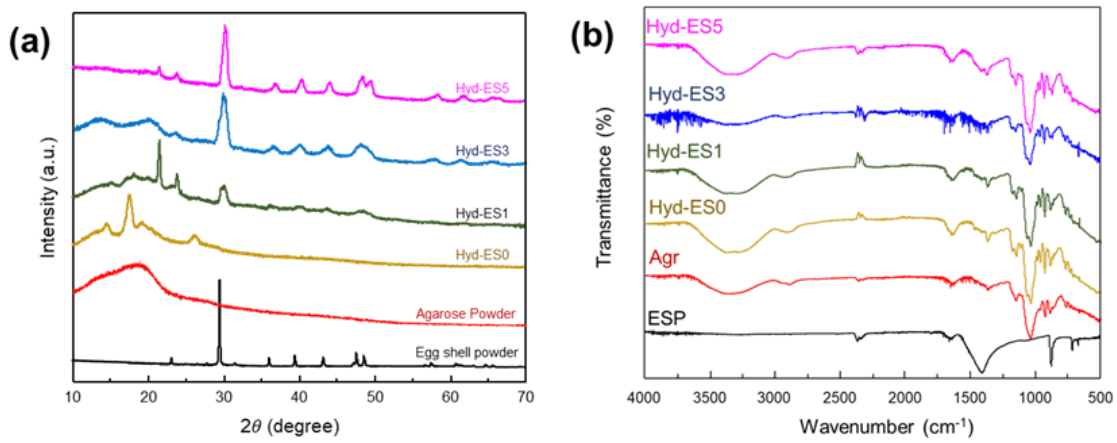

Figure 1. (a) XRD patterns, and (b) FTIR spectra of ESP, Agarose, and Agar-ESP hydrogel.

approach to address water scarcity issues is the application of hydrogels for water gelling [9]. Hydrogels possess a high water absorption and retention capacity, making them a clean and efficient growth medium. Their three-dimensional porous structure creates an optimal environment for seed germination and seedling development [10].

Hydrogels are polymers with a three-dimensional network structure that can retain significant amounts of water and nutrients, making them highly suitable for agricultural applications [11]. Hydrogels have attracted considerable interest as soil conditioners [12], seed coatings [13], and have been employed to regulate the release of fertilizer. Recent studies suggest that natural hydrogels can function as efficient water and nutrient retention media [14]. Unlike commercial synthetic hydrogels, such as polyacrylamide (PAM) or polyacrylate, which are non-biodegradable and may persist in the soil for years or release toxic monomers (e.g., acrylamide), natural polymer-based hydrogels offer a distinct ecological advantage. Agarose-based hydrogels are known to degrade naturally within months due to microbial activity, leaving no harmful residues. Given the increasing interest in sustainable agricultural practices, this biodegradability makes agarose a superior candidate for single-use agricultural cycles compared to their synthetic counterparts.

However, despite their benefits, most pure hydrogels have limited nutrient content, requiring external supplementation to support optimal plant growth, which can reduce their efficiency as standalone growing media. This study introduces a novel approach to valorizing eggshell waste by incorporating it into hydrogels for seedling growth in soilless cultivation. Unlike previous work by Cao and Li [15], who enhanced agarose hydrogels with activated carbon to improve mechanical strength and water retention, we exploit calcium carbonate from eggshells to enhance hydrogel performance. Physicochemical analyses and functional evaluations reveal that eggshell powder acts both as a structural filler and a nutrient carrier, offering added agronomic and ecological value by transforming organic waste into a sustainable raw material for agricultural hydrogels.

Although other researchers have incorporated $CaCO_3$ fillers [16] and various biofillers derived from natural waste into polymer and hydrogel systems, the agarose-egg shell powder (ESP) hydrogel developed in this study exhibits distinct material properties and functional behaviors. ESP is presented as a waste-derived alternative to synthetic $CaCO_3$. Beyond serving as a source of inert $CaCO_3$ (~94–95%), ESP also contains biogenic materials and organic groups (including peptides and proteins) absent in pure $CaCO_3$ fillers [17]. The functional groups of these organic components facilitate more intricate physical interactions than those of pure $CaCO_3$ fillers [18], forming hydrogen bonds with hydroxyl groups in polysaccharides such as agarose, thereby altering swelling, mechanical, and barrier properties compared to systems filled with conventional $CaCO_3$ [17]. Furthermore, ESP integrates more readily into polymers than synthetic calcium carbonate when employed as a filler [19]. These characteristics

enable systematic modulation of water absorption and mechanical responses that diverge from previously reported agarose–$CaCO_3$ or other polysaccharide–$CaCO_3$ systems [20]. In addition to structural reinforcement or sustainability considerations, ESP introduces the potential for gradual availability of Ca^{2+} ions within the hydrogel matrix, supporting multifunctional roles that combine water retention with nutrition-related functions [21]. To the best of our knowledge, such an agarose–ESP system has not been previously reported or evaluated in the context of hydrogel-based plant growth media.

The hydrogel used came from agarose. Agarose is a polysaccharide with repeating disaccharide units. Agarose is extracted from red algae, such as *Gelidium sp.* and *Gracilaria sp*. Although agarose as a raw material is generally more expensive than other natural polymers, it offers several advantageous physicochemical properties. Agarose has a great potential for use in planting media because it is a natural polymer with biodegradable qualities, such as being safe (non-toxic), biocompatible, easy to break down, and easy to integrate into the tissue [22]. Agarose forms thermoreversible hydrogels that dissolve at temperatures above 90 °C and resolidify upon cooling to room temperature, exhibit a well-organized network structure with high water absorption and retention capacity, and can be fabricated without the use of chemical cross-linkers [15]. In contrast, many other natural polymers, such as starch and alginate, require additional components or chemical modifications to form stable hydrogels, which may increase formulation complexity and processing costs [23]. Therefore, despite its higher initial material cost, the intrinsic properties of agarose can reduce overall processing requirements, simplify hydrogel fabrication, lower operational and material costs associated with cross-linking chemistry, and shorten processing time.

We hope that this research will benefit urban communities with limited land availability by enabling agricultural activities through soilless farming systems. By adding eggshell powder compounded with hydrogel to the plant growth medium, this study aims to support high-quality plants with faster growth. Moreover, by adding value to eggshell waste, this research contributes to mitigating the adverse environmental impacts associated with eggshell disposal. Based on the formulation used in this study, approximately 90–330 g of eggshell powder can be valorised per 1 kg of agarose-based hydrogel, depending on the agarose-to-eggshell ratio. This approach promotes waste circularity by transforming an abundant food industry byproduct into a functional agricultural material.

2. MATERIALS AND METHODS

2.1. Materials

Agarose powder (analytical reagent grade) was purchased from Sigma-Aldrich Corporation, with a maximum sulfate content of ≤0.15%, low electroendosmosis (EEO <0.13), and high gel

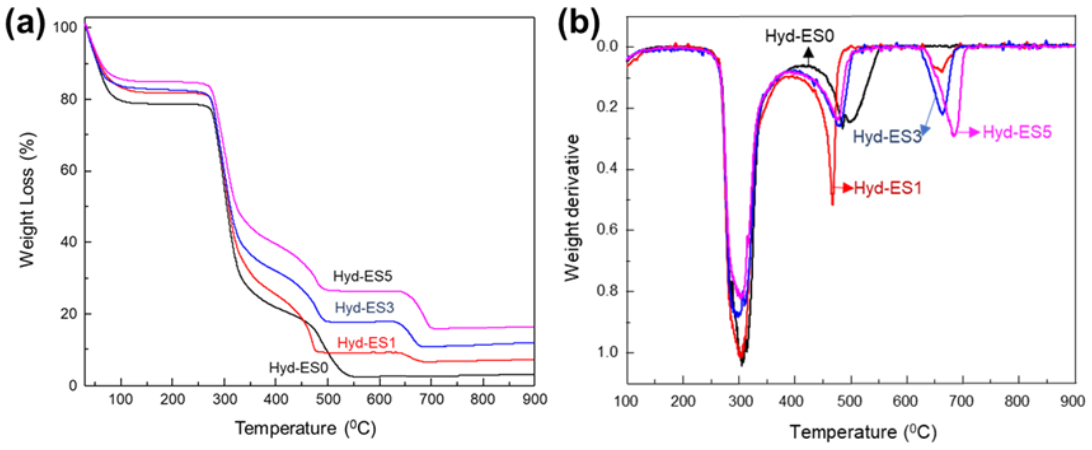

Figure 2. (a) TGA, and (b) DTG curves of Agar-ESP hydrogels.

Table 1. Density of prepared hydrogels.

Sample	Density (g/cm^3)
Hyd-ES0	0.950 ± 0.065
Hyd-ES1	0.992 ± 0.040
Hyd-ES3	0.997 ± 0.068
Hyd-ES5	1.020 ± 0.067

strength (>1.2 kg/cm² at 1.0% w/v). Hybrid broccoli seeds were sourced from Trubus Bina Swadaya Co., Ltd. Deionized (DI) water was prepared in the laboratory, and all chemicals were used as received, without further purification.

2.2. Methods

2.2.1. Preparation of Eggshell Powder (ESP)

The eggshells are first washed with distilled hot water to remove impurities, then cleaned and dried at 70 °C in a hot air oven for 4 h. After drying, they are ground without membrane separation and sieved to obtain particles smaller than 75 µm. The resulting powder is used without any additional chemical or physical processing.

2.2.2. Preparation of Eggshell-filled Hydrogel Composite

The method used in this study was adapted from Cao and Li [16]. Agarose was dissolved in DI water at a concentration of 10 wt% and stirred while gradually adding eggshell powder. The mixture was then subjected to ultrasonication for 1 h at room temperature. Subsequently, it was heated at 95 °C with continuous stirring until the agarose was completely dissolved and the eggshell powder was homogeneously dispersed. The hydrogel-eggshell composite was synthesized using various mass ratios of agarose to ESP, specifically 10:0, 10:1, 10:3, and 10:5, labeled as Hyd-ES0, Hyd-ES1, Hyd-ES3, and Hyd-ES5, respectively. The resulting agarose-eggshell hydrogel solution was then poured into a receptacle and allowed to cool at room temperature, forming the final agarose-eggshell hydrogel.

2.3. Characterization

FTIR spectra of all samples were recorded using an IRSpirit FTIR spectrophotometer (Shimadzu, Japan) to analyze functional groups and molecular interactions. Additionally, the crystalline structures of agarose and the Agar-ESP composite hydrogels were examined via XRD with a Bruker AXS diffractometer (Germany) over a diffraction angle range of 10–70°. The thermal properties of the samples were examined to assess their thermal stability and phase transitions resulting from changes in enthalpy. Thermal analysis was performed using a differential thermal analyzer (Hitachi, STA7200), which provided both thermogravimetric analysis (TGA) and differential scanning calorimetry (DSC) thermograms. The maximum temperature was set to 600 °C, with a heating rate of 10 °C/min. An inert purge gas was used during the characterization process. The surface morphology of the dried hydrogel was examined using a scanning electron microscope (SEM) (HITACHI SU3500, Japan) to analyze its microstructural features, including porosity, surface texture, and internal architecture.

The density of Hyd-ES was calculated by measuring the mass and dimensions of cubic hydrogel samples, using the following Equation 1.

$$\rho = \frac{m}{V} \quad (1)$$

where ρ represents the density, m is the mass, and V is the volume of the hydrogel sample.

The hydrogel's ability to absorb water without dissolving was measured by calculating the degree of swelling, which is the ratio between the water-swollen hydrogel mass (m_2) and the dry hydrogel mass (m_1). The hydrogel was dried at 50 °C in an oven until no further weight reduction was observed, which was achieved after 120 h. The dry hydrogel was then rehydrated in deionized water at 25 °C, and the hydrated mass (m_2) was measured at intervals of 0, 3, 6, 12, 24, and 48 h. The swelling ratio was determined using the following Equation

2.

$$Degree\ of\ swelling\ (\%) = \frac{m_2 - m_1}{m_1} \times 100\% \quad (2)$$

To assess the weight reduction of the hydrogel, a weight loss test was performed. The hydrogel was initially dried at 50 °C for 5 days (Wi). It was then immersed in deionized water at 25 °C for 48 h. Following this, the hydrogel was dried once more at 50 °C for 5 days (Wf). The weight loss was determined using the following Equation 3.

$$Weight\ loss\ (\%) = \frac{W_i - W_f}{W_i} \times 100\% \quad (3)$$

The mechanical properties of the hydrogels were assessed using a Universal Tensile Tester (SM-200, Sinowon, China) at room temperature. The hydrogel samples were shaped into blocks with dimensions of 20 mm × 5 mm × 3 mm. During the test, compressive stress and strain were measured and subsequently plotted. The compression modulus, a key parameter for evaluating the mechanical response of hydrogels to external forces, was calculated by determining the slope of the linear stress-strain curve.

Seedling growth experiments were carried out in a controlled environment using a light incubator to ensure optimal conditions for seed growth. The incubator was maintained at a temperature of 25 ± 2 °C under continuous light exposure, providing consistent illumination to support germination. The relative humidity was regulated at approximately 50% to create a stable and suitable atmosphere for seed development. For the experiment, four different hydrogel-based culture media—Hyd-ES0, Hyd-ES1, Hyd-ES3, and Hyd-ES5—were utilized to assess their effects on seedling growth. Broccoli seeds were evenly distributed on the surface of each culture medium to ensure uniform exposure to nutrients and moisture. Each culture medium contained a total of nine seeds, with three replicates prepared for each condition to ensure statistical reliability and reproducibility of the results.

3. RESULTS AND DISCUSSIONS

3.1. XRD Characterization

The crystal structures of ESP and Agar–ESP hydrogels were examined by XRD analysis. As illustrated in Figure 1(a), the XRD pattern of ESP displays several prominent diffraction peaks located at around 23.1°, 29.48°, 36.08°, 39.47°, 43.21°, 47.51°, and 48.55° (2θ). These peaks are characteristic of calcite $CaCO_3$, confirming that this phase predominates in the eggshell powder. The corresponding interplanar spacing values (d-spacing) were calculated to be 3.55, 3.03, 2.49, 2.28, 2.09, 1.91, and 1.87 Å, which can be indexed to the (012), (104), (110), (113), (202), (018), and (116) planes, respectively. This diffraction pattern closely matches those reported for eggshell-derived $CaCO_3$ in previous studies [24]. The strongest peak at 2θ = 29.48°, associated with the (104) plane, shows a high peak crystallinity degree of 94.6%, suggesting a well-ordered calcite structure, as commonly observed in biogenic $CaCO_3$ materials. Here, the peak crystallinity degree is defined as the ratio of the area of the dominant peak to the total area of the XRD pattern [25]. Agarose exhibited a broad diffuse halo centered around 2θ = 18.4°, which is characteristic of its weakly semi-crystalline or predominantly amorphous structure in the powder form [26]. The XRD pattern of Hyd-ES0 showed broad diffraction features at 14.4°, 17.5°, and 26.3°, reflecting the amorphous nature of the agarose hydrogel matrix. In contrast, the XRD

Table 2. Swelling kinetics parameters modeled using Schott's pseudo-second-order and Ritger-Peppas equations.

Sample	Schott's Second Order			Ritger-Peppas		
	Qeq,theo (%)	ks (g/g·h)	R2	n (Diffusion Exponent)	k	R2
Hyd-ES0	266.4	0.0015	0.999	0.29	0.43	0.994
Hyd-ES1	264.3	0.0012	0.999	0.32	0.42	0.986
Hyd-ES3	222.7	0.0013	0.999	0.37	0.38	0.993
Hyd-ES5	186.4	0.0023	0.999	0.26	0.45	0.979

Table 3. Mechanical properties of Agar-ESP hydrogels.

Sampel	Compressive Modulus (kPa)	Compressive Strength (kPa)	Strain at Failure (%)
Hyd-ES0	113.54	36.67	45.31
Hyd-ES1	84.44	28.91	37.58
Hyd-ES3	68.17	30.04	44.11
Hyd-ES5	44.13	28.17	42.66

patterns of Hyd-ES1, Hyd-ES3, and Hyd-ES5 displayed combined diffraction features originating from both agarose and eggshell powder. Sharp diffraction peaks appearing at around $2\theta \approx 29–30°$ correspond to the (104) plane of calcite $CaCO_3$, indicating the incorporation of crystalline $CaCO_3$ into the hydrogel matrix. The peak crystallinity degree increased from 44.7% (Hyd-ES1) to 59.1% (Hyd-ES3) and 66.5% (Hyd-ES5), suggesting an enhanced contribution of the crystalline calcite phase with increasing ESP content.

3.2. FTIR Spectra

FTIR spectroscopy was utilized to explore the molecular interactions present in ESP, agarose, and Agar-ESP hydrogels. The resulting spectra for ESP, pure agarose hydrogel, and the Agarose-ESP composite hydrogels are presented in Figure 1(b). In the ESP spectrum, FTIR analysis revealed absorption bands in the range of 712–1411 cm^{-1}, corresponding to the vibrational modes of carbonate ions (CO_3^{2-}) within calcium carbonate ($CaCO_3$) [27]. Two prominent peaks at 710 and 876 cm^{-1} were associated with in-plane and out-of-plane bending vibrations of CO_3^{2-}, confirming the presence of $CaCO_3$. A strong band observed near 1421 cm^{-1} was attributed to the asymmetric stretching of the carbonate group, indicating a high abundance of carbonate compounds in the eggshell matrix [28]. Additionally, weak absorptions detected at 2360 and 2357 cm^{-1} were linked to the C=O stretching vibrations of the carbonate [29].

The FTIR spectrum of agarose exhibits intermolecular hydrogen bonding and OH stretching vibrations at 1645 and 3000–3500 cm^{-1}, respectively [15]. The asymmetric and symmetric stretching vibrations of CH_2 are detected at 2949 and 2894 cm^{-1}, respectively [30]. Additionally, the peaks observed at 772, 887, and 931 cm^{-1} are associated with the 3,6-anhydro-β-galactose structure [31], while the peaks at 1047 and 1152 cm^{-1} correspond to the glycosidic linkages and -C-O-C- bond, respectively. The FTIR spectrum of Hyd-ES0 showed absorption peaks between 3600 and 3200 cm^{-1}, corresponding to –OH stretching vibrations, indicating hydrogen bonding within the hydrogel. A peak at 1071 cm^{-1} is linked to –OH bending, while the peak at 1158 cm^{-1} corresponds to C–O–C stretching vibrations. Additionally, bands at 773, 894, and 929 cm^{-1} are associated with the skeletal bending of the 3,6-anhydro-β-galactose structure, confirming the structural integrity of agarose in the hydrogel matrix.

During the synthesis of the Hyd-ES composite, no new covalent bonds were detected, as evidenced by the absence of additional absorption peaks and the close similarity between the FTIR spectra of the Hyd-ES composites and pure agarose. This observation suggests that no chemical modification occurred during composite formation [32]. However, a gradual shift of the O–H stretching band toward lower wavenumbers (red shift) was observed, indicating the presence of physical interaction between agarose and ESP [33]. The characteristic O–H stretching peak of agarose powder at 3338 cm^{-1} shifted to approximately 3310 cm^{-1} in the agarose hydrogel (Hyd-ES0) and further to 3294 cm^{-1} upon increasing ESP content (Hyd-ES5). The red shift reflects the strengthening of hydrogen bonds between the hydroxyl groups of agarose and the carbonate-rich surfaces of the eggshell powder. Meanwhile, the O–H bending vibration around 1635 cm^{-1} remains nearly unchanged across all Hyd-ES samples, indicates that the hydration environment associated with bound water is largely preserved after gelation and ESP incorporation [34]. The overall similarity of the spectral profiles, together with these subtle shifts, confirms that ESP is successfully embedded within the agarose matrix through physical

interactions without inducing chemical modification of the polymer backbone.

3.3. Thermal Behavior

TGA and DSC profiles provide insight into the thermal characteristics of hydrogels incorporating eggshell powder, revealing distinct multi-step degradation patterns and thermal transition events. As shown in Figure 2(a), the TGA curves for Hyd-ES0, Hyd-ES1, Hyd-ES3, and Hyd-ES5 were obtained under a nitrogen atmosphere with a controlled heating rate of 10 °C/min. All hydrogel samples exhibited a four-stage weight loss pattern, except for Hyd-ES0, which underwent only three stages. The initial weight loss, occurring between approximately 30 and 154 °C, is attributed to the evaporation of absorbed water molecules. The second and third weight loss stages, observed within the temperature ranges of 154 to 408 °C and 408 to 510 °C, are associated with the breakdown of side groups, the collapse of the gel network, and the degradation of the polysaccharide skeleton. The final weight loss stage, occurring between 510 and 700 °C, corresponds to the thermal decomposition of $CaCO_3$, leading to CO_2 release [27]. As the moisture evaporates, an increase in ESP content results in a gradual rise in the decomposition temperature of the hydrogels. Hyd-ES0 decomposes at 476 °C, while Hyd-ES5 degrades at 548 °C. This delay in degradation is likely due to the enhanced thermal stability of ES, which provides heat insulation and slows down the decomposition of agarose [15].

The DSC profiles shown in Figure 2(b) corroborate these thermal transitions, where the endothermic peaks are associated with polymer decomposition and the release of volatiles, while the exothermic peaks are indicative of crystallization or potential crosslinking reactions. Variations in both the intensity and position of these peaks among the samples point to differences in their physicochemical characteristics, shaped by the presence of eggshell-derived constituents. These findings highlight the contribution of eggshell

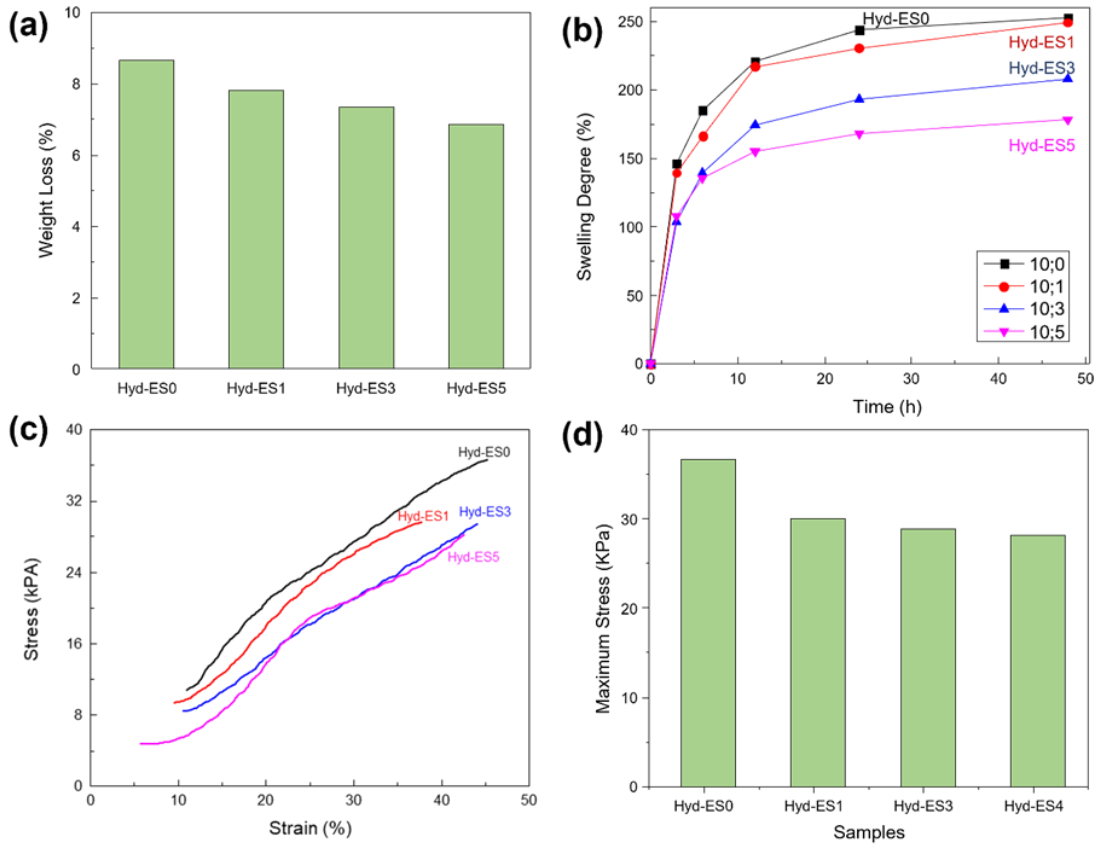

Figure 3. (a) Swelling degree, (b) Weight loss (c) compressive strain-stress curves of Hyd-ES0, Hyd-ES1, Hyd-ES3, Hyd-ES5, and (d) Maximum Stress.

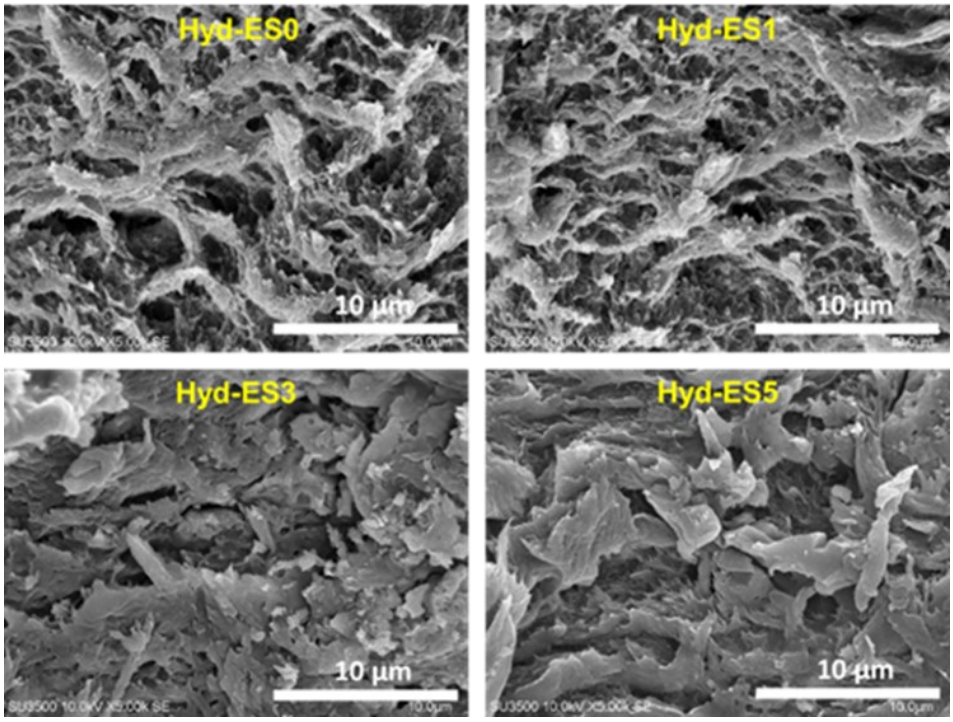

Figure 4. SEM images of prepared hydrogels.

powder in improving the thermal stability and reinforcing the structural integrity of the hydrogel systems.

3.4. Density

The density of a hydrogel is a key parameter governing its mechanical strength and elasticity. Excessively dense networks tend to exhibit reduced flexibility and diminished capacity to respond to environmental variations, whereas low-density structures often lack the structural integrity required to retain their shape. Table 1 presents the density of Hyd-ES for all variations. The density of Hyd-ES increases with the rising ES concentration in the hydrogel. Hydrogel density affects its ability to absorb water and swell. Low-density hydrogels exhibit high water absorption capacity due to their large pore structures and abundant inter-crosslinking spaces. Hyd-ES5 has the highest density because of the high eggshell content. The addition of eggshell increases the solution's density, which can hinder the dynamic movement of solvent molecules. An optimal hydrogel density facilitates efficient water retention while preventing both waterlogging and excessive drainage. When formulated at the appropriate density, hydrogels can preserve porosity, thereby ensuring adequate oxygen supply to plant roots, a critical factor for promoting healthy growth.

3.5. Weight Loss and Swelling Degrees

The swelling degree of Hyd-ES decreased with increasing ESP concentration, as shown in Figure 3 (a). All Hyd-ES samples exhibited significant water absorption from 0 to 24 h. Swelling continued up to 48 h, though the increase was not significant. The Hyd-ES0 sample had the highest swelling degree at 252.7 ± 18.7%, followed by Hyd-ES1 at 249.2 ± 20.4%, Hyd-ES3 at 207.7 ± 6.2%, and Hyd-ES5 at 178.3 ± 4.8% after 48 h of immersion.

The reduction in the swelling degree of Hyd-ES hydrogels is attributed to the increased network density and the physical restrictions imposed by the ESP filler. To elucidate the water uptake mechanism, the swelling kinetics were analyzed using Schott's pseudo-second-order model and the Ritger–Peppas empirical equation, both of which are widely employed to describe swelling behavior in crosslinked polymer networks [35][36]. The calculated kinetic parameters are summarized in Table 2. The high correlation coefficients (R^2 > 0.99) obtained for all formulations indicate that the swelling process follows pseudo-second-order kinetics, suggesting that water absorption is governed by the availability of free sorption sites within the hydrogel matrix rather than by simple

diffusion alone [35][37].

According to the Ritger–Peppas model ($M_t/M_{eq} = kt^n$), the diffusion exponent (n) values for all samples ranged from 0.26 to 0.37 (Table 2). These values are below 0.5, which is characteristic of less-Fickian (pseudo-Fickian) diffusion behavior, where the rate of water penetration into the hydrogel is slower than polymer chain relaxation and therefore becomes the rate-limiting step [36][38]. Notably, Hyd-ES5 exhibited the lowest n value (0.26) and the lowest equilibrium swelling capacity. This behavior indicates that the incorporation of rigid ESP particles significantly restricts polymer chain mobility, effectively increasing the crosslink density of the network in accordance with the Flory –Rehner swelling theory [39]. In addition, the high filler loading introduces a pronounced tortuosity effect, reducing pore connectivity and obstructing the microscopic pathways required for efficient water diffusion, as commonly reported for particle-filled hydrogel systems [40].

Figure 3(b) illustrates the decrease in weight loss of Hyd-ES. The significant reduction in hydrogel weight indicates that the polymer structure degraded, losing its integrity and strength. This weight loss reflects the remaining gel fraction after prior dissolution in deionized water. During the swelling test, the polymer chains expanded as deionized water entered the hydrogel network, allowing bioactive compounds to diffuse out of the hydrogel structure [41]. A denser hydrogel network with an elevated eggshell content limits the diffusion of incorporated additives or active compounds, thereby moderating and regulating the rate of weight loss. Among the tested formulations, Hyd-ES5 demonstrated the lowest weight reduction at 6.8 ± 0.2%, reflecting its superior ability to retain structural integrity. The higher the eggshell content, the lower the hydrogel's weight reduction. For Hyd-ES0, weight loss was recorded at 8.6 ± 0.7%, followed by Hyd-ES1 at 7.8 ± 0.4%, and Hyd-ES3 at 7.3 ± 0.7%. These results align with the study by Cao and Li [15], where the weight loss curve decreased as the concentration of activated carbon in agarose hydrogel increased.

3.6. Mechanical Properties

The mechanical properties of Agar-ESP composite hydrogels are represented by the stress-strain curve as shown in Figure 3(c), which

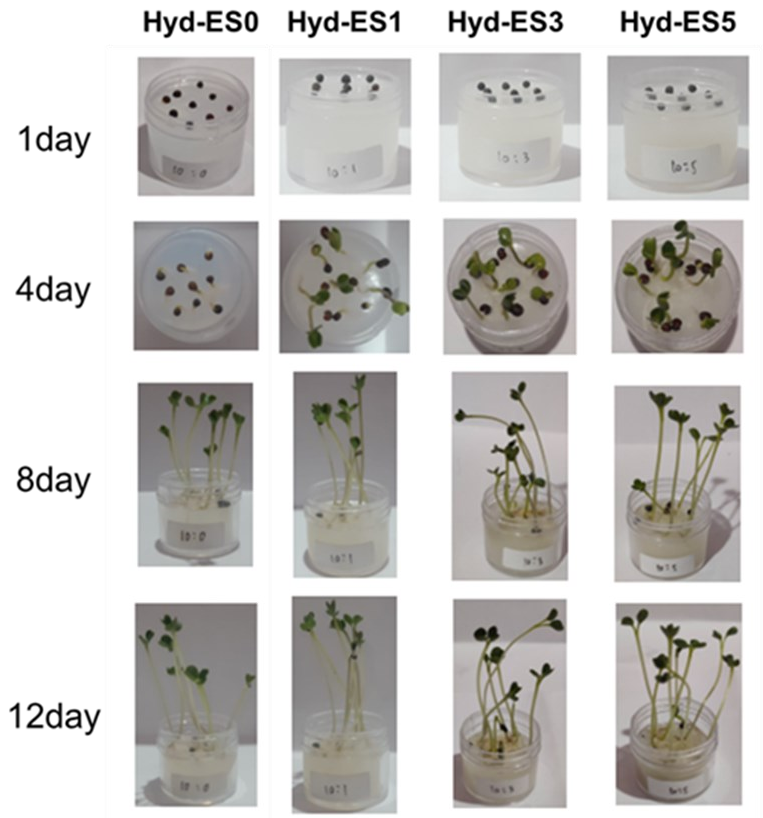

Figure 5. Photograph of broccoli seedling growth test on Hyd-ES0, Hyd-ES1, Hyd-ES3, and Hyd-ES5.

illustrates the relationship between the force applied (stress) on the hydrogel and the resulting deformation (strain). The stress-strain characteristics of the Agar-ESP composite hydrogels exhibit unique features, like previous reports, with a sharp, exponential J-shaped stress increase [15][42]. The distinct J-shaped curve is attributed to the hydrogel's water-rich structure. The initial linear region of the curve reflects the hydrogel's elastic deformation, where the material returns to its original shape when the applied force is removed, by Hooke's law. As the force increases, the curve takes on a J-shaped exponential form, indicating the hydrogel's viscoelastic behavior, where deformation becomes permanent due to the breaking of hydrogen bonds.

The addition of ESP concentration in the hydrogel decreases its compressive strength. Table 3 summarizes the quantitative mechanical properties, including compressive modulus and maximum stress (stress-at-failure), for all hydrogel variations. Figure 3(d) visually confirms the trend where the mechanical integrity generally declines with higher ESP content. The observed reduction is attributed to weak interfacial adhesion between the hydrophilic agarose matrix and the rigid, inorganic ESP particles. As seen in the surface SEM images (Figure 4), the incorporation of ESP disrupts the continuity of the porous agarose network. Rather than reinforcing the matrix through chemical cross-linking, the ESP particles act as structural defects and stress concentrators. Under compressive load, the lack of strong polymer-filler adhesion prevents efficient stress transfer, causing the hydrogel to fail at lower stress values compared to the pure agarose network [43][44]. The significant decrease in compressive modulus (from 113.5 kPa in Hyd-ES0 to 44.1 kPa in Hyd-ES5) further confirms that the filler particles interrupt the elastic polymer chains, limiting the network's ability to resist deformation [45].

3.7. SEM Images

The morphologies of Hyd-ES0, Hyd-ES1, Hyd-ES3, and Hyd-ES5 were examined via SEM to investigate the microstructural characteristics of Agar-ESP composite hydrogels, as presented in Figure 4. The images reveal distinct structural variations among the samples, which are directly relevant to their potential use as plant growth media. Hyd-ES0, consisting solely of agarose, displays a highly porous and interconnected network that promotes efficient water absorption and diffusion. With the incorporation of ESP (Hyd-ES1 to Hyd-ES5), the surface becomes rougher and porosity decreases [46][47]. From an application perspective, Hyd-ES0 provides robust structural support but allows faster water drainage, whereas ESP-containing hydrogels, despite lower mechanical strength, enable more controlled water retention due to their reduced porosity. Beyond structural modification, ESP also enriches the hydrogel with essential nutrients, particularly calcium and trace minerals, which are vital for cell wall formation, root elongation, and overall plant health [48][49]. Thus, achieving an optimal balance between porosity, mechanical performance, and nutrient content is critical for developing hydrogel-based planting media capable of ensuring adequate water retention while enhancing plant nutrition and structural stability.

3.8. Seedling Growth

Figure 5 displays the seedling growth observed on the Agar–ESP composite hydrogels. Seeds placed on the surface of the ESP-containing hydrogels began germinating within 4 days. Quantitative analysis of seedling height (Figure 6 (a)) reveals that Hyd-ES1 achieved the highest growth rate. Statistical analysis using One-Way ANOVA confirmed a significant difference in plant height at day 11 across the groups ($p < 0.05$). Specifically, an independent t-test showed that seedlings grown in Hyd-ES1 (mean height: 3.03 cm) were significantly taller than those in the control Hyd-ES0 (mean height: 2.07 cm) with a p-value of 0.016.

Error bars in Figures 6(a) and 6(c) represent the standard error of the mean (SEM) derived from a sample size of n = 41–45 individual plants, demonstrating robust statistical power. Although direct quantification of calcium leaching was not conducted, the biological data suggests a trade-off between nutritional benefits and physical constraints, as commonly reported for nutrient-enriched hydrogel systems used in plant growth media [50][51]. The superior growth in Hyd-ES1 suggests an optimal balance where the bioavailable

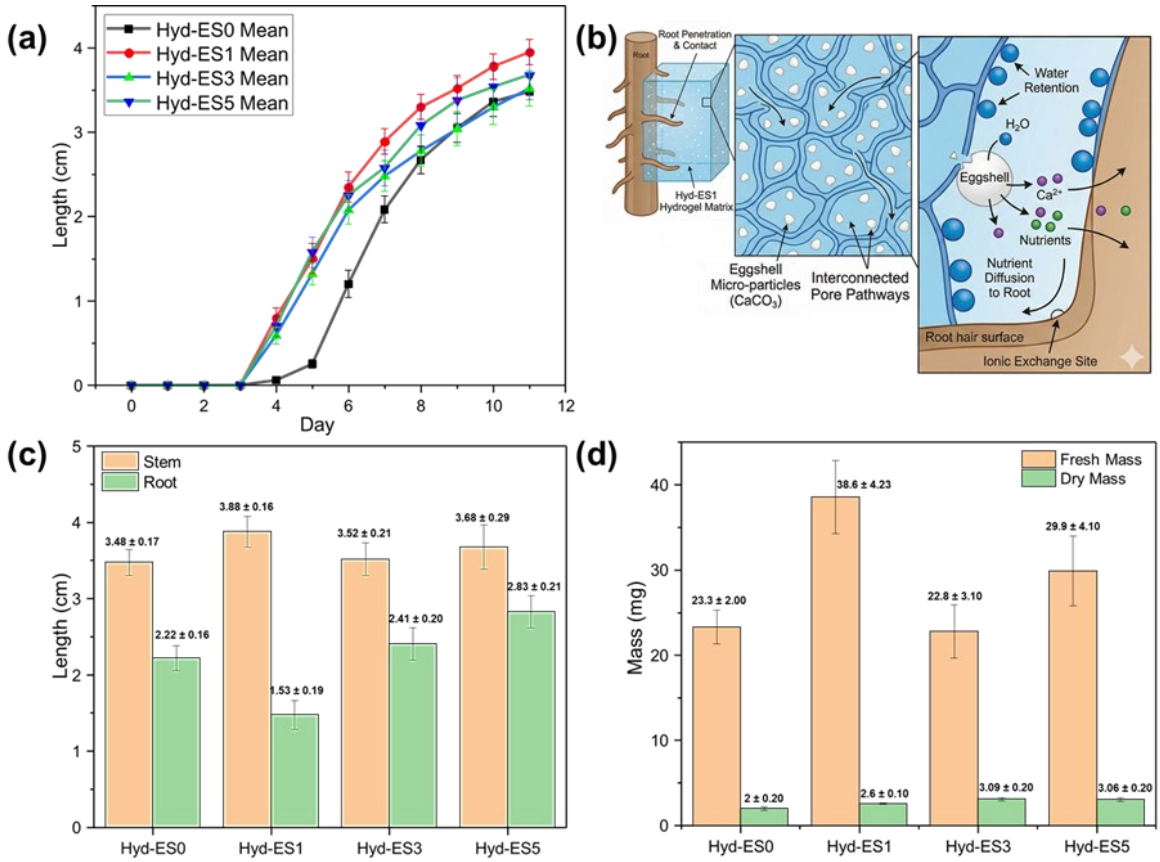

Figure 6. (a) The seedling growth of broccoli seeds, (b) Mechanism of seedling growth, (c) root and stem length of seedlings and (d) fresh and dry weight of seedlings in Hyd-ES0, Hyd-ES1, Hyd-ES3, Hyd-ES5.

calcium from ESP aids development without severely restricting root penetration, consistent with previous findings on moderate filler loading in hydrogel-based substrates [51]. Conversely, in Hyd-ES5, despite potentially higher calcium content, the significant increase in crosslink density and stiffness (as shown in swelling and mechanical data) physically restricted root elongation, resulting in lower biomass compared to Hyd-ES1, in agreement with reports on the inhibitory effects of increased matrix rigidity and tortuosity on root growth [52][53].

Among all formulations, Hyd-ES1 containing a low concentration of ESP exhibited the most favorable performance in promoting root and shoot growth. As illustrated in Figure 6(c), seedlings grown in Hyd-ES1 developed significantly longer roots and stems compared to those cultivated in other media. This observation indicates that a lower ESP concentration may provide a more balanced environment for root and shoot development. The improved performance of Hyd-ES1 is attributed to a synergistic balance between physical structure and nutrient bioavailability. Mechanistically, nutrient supply is governed by the interaction between plant roots and the ESP filler dispersed within the hydrogel matrix. Although the bulk hydrogel remains chemically neutral, plant roots actively modify their immediate environment (the rhizosphere) through the exudation of protons and low-molecular-weight organic acids, a well-established process that induces localized acidification and enhances mineral dissolution in soils. This rhizosphere-driven acidification facilitates the partial dissolution of $CaCO_3$ particles embedded in the matrix, leading to the gradual release of bioavailable Ca^{2+} ions, as schematically illustrated in Figure 6(b) [54][55].

In Hyd-ES1, the hydrogel network remains sufficiently porous (as confirmed by SEM observations and swelling behavior) to permit efficient water diffusion and root penetration, thereby enabling plant roots to access the released Ca^{2+} ions effectively. Similar structure–function relationships have been reported for biodegradable hydrogel systems, where moderate filler loading

preserves pore connectivity and mass transport while supporting nutrient delivery [50][51]. In contrast, samples with higher ESP content (Hyd-ES3 and Hyd-ES5) exhibit diminished performance due to physical limitations. The increased filler density raises the tortuosity of diffusion pathways and generates a stiffer, more compact network that mechanically restricts root elongation and proliferation. Under such conditions, nutrient accessibility becomes diffusion-limited, and calcium uptake is hindered despite the potential occurrence of $CaCO_3$ dissolution [52][53]. Consequently, Hyd-ES1 represents a critical compositional threshold at which Ca^{2+} ion availability is maximized without sacrificing the physical permeability and mechanical compliance necessary for root expansion and effective nutrient acquisition.

Interestingly, despite higher calcium content in Hyd-ES3 and Hyd-ES5 due to increased ESP concentrations, these samples did not result in better growth outcomes. SEM images revealed that higher ESP content tended to produce denser and more layered structures, which may hinder root penetration and reduce aeration within the hydrogel. This suggests that Hyd-ES1 may represent an optimal balance between nutrient provision, structural support, and aeration [56]–[58]. Furthermore, fresh and dry biomass data presented in Figure 6(d) reinforce this finding. Plants grown in Hyd-ES1 exhibited significantly higher fresh and dry weights than those grown in other media, underscoring the beneficial effects of moderate ESP addition. This enhancement in growth can be attributed to the synergistic role of ESP in improving water-holding capacity, contributing calcium a crucial nutrient for cell wall development and modifying the polymer network to support plant development [57]–[61]. These results demonstrate that the Agar–ESP composite hydrogel with a low ESP concentration (Hyd-ES1) effectively supports seedling growth. This material holds considerable promise for agricultural applications, particularly as an alternative growth medium in resource-limited or controlled-environment cultivation systems.

Beyond its superior performance in supporting seedling growth, the Agar–ESP hydrogel also presents important sustainability implications. Eggshells are a major food-industry byproduct and have been widely reported as promising candidates for waste valorisation into value-added materials, supporting circular economy approaches in material development [1][2]. Based on the formulation employed in this study, approximately 90–330 g of eggshell powder can be valorised per kilogram of agarose-based hydrogel, depending on the agarose-to-eggshell ratio. Agarose itself is a naturally derived and biodegradable polysaccharide obtained from marine biomass [62]. Previous studies have reported that biodegradable polysaccharide-based hydrogels used in agricultural applications generally undergo gradual degradation over weeks to months under environmental conditions, in contrast to persistent synthetic polymers [9][43].

Compared to conventional commercial hydrogels, such as polyacrylamide-based systems derived from petroleum resources, the Agar–ESP hydrogel offers clear environmental advantages, including improved biodegradability and a reduced risk of long-term polymer accumulation in soil. Polyacrylamide-based hydrogels are known to exhibit limited biodegradability and may raise environmental concerns related to polymer persistence and potential residual toxicity [44][45]. Although a comprehensive life cycle assessment was beyond the scope of this study, the use of renewable raw materials, low-energy fabrication processes, and eggshell waste valorisation suggests a lower environmental footprint and good scalability for agricultural applications, particularly in small-scale and urban farming systems [57][58][60].

4. CONCLUSIONS

We have successfully developed Agar-ESP hydrogel through mechanical blending techniques. The increase in ESP concentration resulted in a decrease in pore size, swelling capacity, and weight loss of the hydrogel. FTIR results identified the functional groups from both agarose powder and ESP, confirming their integration within the Agar-ESP hydrogel. XRD analysis indicated that the crystalline calcite structure of ESP and the semi-crystalline matrix of agarose remained intact after hydrogel formation. TGA analysis showed that incorporating ESP improved the thermal stability of

the Agar-ESP composite hydrogel. Additionally, higher ESP concentrations increased the density of cross-linking between agarose and ESP, though this was accompanied by a reduction in the maximum compressive strength of the hydrogel. Based on our findings, the Agar-ESP hydrogel, particularly Agas-ES1, demonstrates remarkable potential as an effective medium for seed germination and plant growth. This makes it a promising alternative to conventional growth media, offering a sustainable and innovative solution for agricultural and horticultural applications.

AUTHOR INFORMATION

Corresponding Author

Ade Yeti Nuryantini — Master's Program in Science Education, UIN Sunan Gunung Djati Bandung, Bandung-40614 (Indonesia); Department of Physics Education, UIN Sunan Gunung Djati Bandung, Bandung-40614 (Indonesia); Department of Physics, UIN Sunan Gunung Djati Bandung, Bandung-40614 (Indonesia);
orcid.org/0000-0001-6382-7249
Email: ade.yeti@uinsgd.ac.id

Authors

Ea Cahya Septia Mahen — Department of Physics Education, UIN Sunan Gunung Djati Bandung, Bandung-40614 (Indonesia);
orcid.org/0000-0002-4131-8723

Indri Oktaviani — Department of Physics, UIN Sunan Gunung Djati Bandung, Bandung-40614 (Indonesia);
orcid.org/0009-0002-3541-0926

Bebeh Wahid Nuryadin — Department of Physics, UIN Sunan Gunung Djati Bandung, Bandung-40614 (Indonesia);
orcid.org/0000-0002-6653-4174

Dhewa Edikresnha — Department of Physics, Institut Teknologi Bandung, Bandung-40132 (Indonesia); Bioscience and Biotechnology Research Center, Institut Teknologi Bandung, Bandung-40132 (Indonesia);
orcid.org/0000-0001-6203-4343

Khairurrijal Khairurrijal — Department of Physics, Institut Teknologi Bandung, Bandung-40132 (Indonesia); Bioscience and Biotechnology Research Center, Institut Teknologi Bandung, Bandung-40132 (Indonesia); Department of Physics, Institut Teknologi Sumatera, Lampung-35365 (Indonesia); Center for Green and Sustainable Materials, Institut Teknologi Sumatera, Lampung-35365 (Indonesia);
orcid.org/0000-0002-9452-4192

Author Contributions

Conceptualization, A. Y. N. and E. C. S. M.; Methodology, A. Y. N., E. C. S. M., and I. O.; Validation, D. E., and K. K.; Formal Analysis, Writing – Original Draft Preparation, and Funding Acquisition, A. Y. N.; Investigation, B. W. N.; Resources, D. E., and K. K.; Writing – Review & Editing, E. C. S. M., D. E., and K. K.; Visualization, E. C. S. M.; Supervision, K. K.; Project Administration, I. O.

Conflicts of Interest

The authors declare no conflict of interest.

ACKNOWLEDGEMENT

This research supported by the Ministry of Religious Affairs Republic Indonesia through the Applied Research for National Development program BOPTN UIN Sunan Gunung Djati Bandung [No.5794/Un.05/V.2/TL.03/12/2022].

DECLARATION OF GENERATIVE AI

During the preparation of this work, the authors used ChatGPT (OpenAI) to assist in refining the writing for clarity and grammar.

REFERENCES

[1] T. A. E. Ahmed, G. Kulshreshtha, and M. T. Hincke. (2019). In: "Food Chemistry, Function and Analysis". 359-397. 10.1039/9781788013833-00359.

[2] C. M. M. Cordeiro and M. T. Hincke. (2012). "Recent Patents on Eggshell: Shell and Membrane Applications". *Recent Patents on Food, Nutrition and Agriculture.* **3** (1): 1-8. 10.2174/2212798411103010001.

[3] M. Gaonkar and A. P. Chakraborty. (2016).

"Application of Eggshell as Fertilizer and Calcium Supplement Tablet". *International Journal of Innovative Research in Science, Engineering and Technology.* **5** (3): 3520-3525. 10.15680/IJIRSET.2016.0503183.

[4] B. J. van Goor. (1968). "The Role of Calcium and Cell Permeability in the Disease Blossom -End Rot of Tomatoes". *Physiologia Plantarum.* **21** (5): 1110-1121. 10.1111/j.1399-3054.1968.tb07339.x.

[5] G. E. Barrett, P. D. Alexander, J. S. Robinson, and N. C. Bragg. (2016). "Achieving Environmentally Sustainable Growing Media for Soilless Plant Cultivation Systems: A Review". *Scientia Horticulturae.* **212** : 220-234. 10.1016/j.scienta.2016.09.030.

[6] D. Massa, J. J. Magan, F. F. Montesano, and N. Tzortzakis. (2020). "Minimizing Water and Nutrient Losses from Soilless Cropping in Southern Europe". *Agricultural Water Management.* **241** : 106395. 10.1016/j.agwat.2020.106395.

[7] H. Soffer, D. W. Burger, and J. H. Lieth. (1991). "Plant Growth and Development of Chrysanthemum and Ficus in Aero-Hydroponics: Response to Low Dissolved Oxygen Concentrations". *Scientia Horticulturae.* **45** (3): 287-294. 10.1016/0304-4238(91)90074-9.

[8] J. Suhl, B. Oppedijk, D. Baganz, W. Kloas, U. Schmidt, and B. van Duijn. (2019). "Oxygen Consumption in Recirculating Nutrient Film Technique in Aquaponics". *Scientia Horticulturae.* **255** : 281-291. 10.1016/j.scienta.2019.05.033.

[9] R. Vundavalli, S. Vundavalli, M. Nakka, and D. S. Rao. (2015). "Biodegradable Nano-Hydrogels in Agricultural Farming: Alternative Source for Water Resources". *Procedia Materials Science.* **10** : 548-554. 10.1016/j.mspro.2015.06.005.

[10] L. Xie, M. Liu, B. Ni, and Y. Wang. (2012). "Utilization of Wheat Straw for the Preparation of Coated Controlled-Release Fertilizer with the Function of Water Retention". *Journal of Agricultural and Food Chemistry.* **60** (28): 6921-6928. 10.1021/jf3001235.

[11] H. Omidian, J. G. Rocca, and K. Park. (2005). "Advances in Superporous Hydrogels". *Journal of Controlled Release.* **102** (1): 3-12. 10.1016/j.jconrel.2004.09.028.

[12] M. M. Ghobashy, H. A. El-Wahab, M. A. Ismail, A. Naser, F. Abdelhai, B. K. El-Damhougy, N. Nady, A. S. Meganid, and S. A. Alkhursani. (2020). "Characterization of Starch-Based Three-Component Gamma-Ray Cross-Linked Hydrogels to Be Used as a Soil Conditioner". *Materials Science and Engineering B: Advanced Functional Solid-State Materials.* **260** : 114645. 10.1016/j.mseb.2020.114645.

[13] Y. Gao, S. Pan, G. Guo, Q. Gu, R. Pan, Y. Guan, and J. Hu. (2020). "Preparation of a Thermoresponsive Maize Seed Coating Agent Using Polymer Hydrogel for Chilling Resistance and Anti-Counterfeiting". *Progress in Organic Coatings.* **139** : 105452. 10.1016/j.porgcoat.2019.105452.

[14] Y. Wu, S. Li, and G. Chen. (2023). Hydrogels as water and nutrient reservoirs in agricultural soil: a comprehensive review of classification, performance, and economic advantages. *Environment Development and Sustainability*. **26** (10): 24653–24685. 10.1007/s10668-023-03706-y.

[15] L. Cao and N. Li. (2021). "Activated-Carbon-Filled Agarose Hydrogel as a Natural Medium for Seed Germination and Seedling Growth". *International Journal of Biological Macromolecules.* **177** : 383-391. 10.1016/j.ijbiomac.2021.02.097.

[16] Y. Gong, Y. Zhang, Z. Cao, F. Ye, Z. Lin, and Y. Li. (2019). "Development of CaCO3 Microsphere-Based Composite Hydrogel for Dual Delivery of Growth Factor and Ca to Enhance Bone Regeneration". *Biomaterials Science.* **7** (9): 3614-3626. 10.1039/C9BM00463G.

[17] E. S. Bhagavatheswaran, A. Das, H. Rastin, H. Saeidi, S. H. Jafari, H. Vahabi, F. Najafi, H. A. Khonakdar, K. Formela, M. Jouyandeh, P. Zarrintaj, and M. R. Saeb. (2019). "The Taste of Waste: The Edge of Eggshell Over Calcium Carbonate in Acrylonitrile Butadiene Rubber". *Journal of Polymers and the Environment.* **27** (11): 2478-2489.

10.1007/s10924-019-01530-y.

[18] T. Li, R. Li, H. Luo, L. Peng, J. Wang, S. Li, M. Zhou, X. Yuan, Z. Zhang, and H. Wu. (2024). "Eggshell Powder as a Bio-Filler for Starch and Gelatin: Ternary Biodegradable Composite Films Manufactured by Extrusion Compression Molding". *Food Hydrocolloids.* **150** : 109632. 10.1016/j.foodhyd.2023.109632.

[19] Z. Zhang, N. Li, L. Sun, Z. Liu, Y. Jin, Y. Xue, B. Li, H. Xuan, and H. Yuan. (2024). "Eggshell Membrane Powder Reinforces Adhesive Polysaccharide Hydrogels for Wound Repair". *International Journal of Biological Macromolecules.* **269** : 131879. 10.1016/j.ijbiomac.2024.131879.

[20] J. Choi, J. Lee, M. E. Shin, S. Been, D. H. Lee, and G. Khang. (2020). "Eggshell Membrane/Gellan Gum Composite Hydrogels with Increased Degradability, Biocompatibility, and Anti-Swelling Properties for Effective Regeneration of Retinal Pigment Epithelium". *Polymers.* **12** (12): 2941. 10.3390/polym12122941.

[21] Z. Zhang, Y. Liu, Y. Gao, J. Huo, S. Dong, L. Liu, and S. Li. (2025). "Sustained-Release Effect of Eggshell Powder Microcapsules on Lavender Essential Oil". *Journal of Food Engineering.* **387** : 112322. 10.1016/j.jfoodeng.2024.112322.

[22] J. Lin, G. Jiao, and A. Kermanshahi-Pour. (2022). "Algal Polysaccharides-Based Hydrogels: Extraction, Synthesis, Characterization, and Applications". *Marine Drugs.* **20** (5): 306. 10.3390/md20050306.

[23] S. Li, F. Yao, Q. Liu, C. Tang, Y. Zhuo, M. Dai, Q. Lv, and X. Zhong. (2025). "Natural Polysaccharide Hydrogels: Design, Preparation, and Tissue Engineering Applications". *Materials & Design.* **259** : 114876. 10.1016/j.matdes.2025.114876.

[24] S. Seesanong, C. Seangarun, B. Boonchom, N. Laohavisuti, W. Boonmee, P. Rungrojchaipon, and P. Phimsirikul. (2024). "Sustainable Production and Physicochemical Characteristics of Calcium Sulfate Dihydrate Prepared from Waste Eggshells". *Crystals.* **14** (7): 577. 10.3390/cryst14070577.

[25] K. Kusjuriansah, M. Rodhiyah, N. A. Syifa, H. R. Luthfianti, W. X. Waresindo, D. A. Hapidin, T. Suciati, D. Edikresnha, and K. Khairurrijal. (2024). "Composite Hydrogel of Poly(Vinyl Alcohol) Loaded by Citrus Hystrix Leaf Extract, Chitosan, and Sodium Alginate with In Vitro Antibacterial and Release Test". *ACS Omega.* 10.1021/acsomega.3c10143.

[26] N. Kerru, L. Gummidi, S. V. H. S. Bhaskaruni, S. N. Maddila, and S. B. Jonnalagadda. (2020). "One-Pot Green Synthesis of Novel 5,10-Dihydro-1H-Pyrazolo[1,2-b]Phthalazine Derivatives with Eco-Friendly Biodegradable Eggshell Powder as Efficacious Catalyst". *Research on Chemical Intermediates.* **46** (6): 3067-3083. 10.1007/s11164-020-04135-6.

[27] K. Naemchan, S. Meejoo, W. Onreabroy, and P. Limsuwan. (2008). "Temperature Effect on Chicken Egg Shell Investigated by XRD, TGA and FTIR". *Advanced Materials Research.* **55** : 333-336. 10.4028/www.scientific.net/AMR.55-57.333.

[28] M. S. Tizo, L. A. V. Blanco, A. C. Q. Cagas, B. R. B. D. Cruz, J. C. Encoy, J. V. Gunting, R. O. Arazo, and V. I. F. Mabayo. (2018). "Efficiency of Calcium Carbonate from Eggshells as an Adsorbent for Cadmium Removal in Aqueous Solution". *Sustainable Environment Research.* **28** (6): 326-332. 10.1016/j.serj.2018.09.002.

[29] G. Pandey, K. N. Dhakal, A. K. Singh, S. K. Dhungel, and R. Adhikari. (2021). "Facile Methods of Preparing Pure Hydroxyapatite Nanoparticles in Ordinary Laboratories". *BIBECHANA.* **18** (1): 83-90. 10.3126/bibechana.v18i1.29600.

[30] S. S. Garakani, M. Khanmohammadi, Z. Atoufi, S. K. Kamrava, M. Setayeshmehr, R. Alizadeh, F. Faghihi, Z. Bagher, S. M. Davachi, and A. Abbaspourrad. (2020). "Fabrication of Chitosan/Agarose Scaffolds Containing Extracellular Matrix for Tissue Engineering Applications". *International Journal of Biological Macromolecules.* **143** : 533-545. 10.1016/j.ijbiomac.2019.12.040.

[31] S. Wang, R. Zhang, Y. Yang, S. Wu, Y. Cao, A. Lu, and L. Zhang. (2018). "Strength

Enhanced Hydrogels Constructed from Agarose in Alkali/Urea Aqueous Solution and Their Application". *Chemical Engineering Journal.* **331** : 177-184. 10.1016/j.cej.2017.08.118.

[32] P. S. Neto, J. B. De Oliveira, R. S. De O Buzatti, V. M. Ferreira, P. P. De Souza, F. D. Chaves, A. S. C. Netto, A. M. M. S. Lameirão, C. A. M. Gomes, D. C. Morgado, M. B. S. Maia, R. F. G. Lima, V. S. Cruz, P. S. De O Patricio, and Â. R. De Oliveira. (2025). "Properties Evaluation of Polyester Composites with Fillers for Electrical Sector Applications". *Journal of Materials Science: Composites.* **6** (1): 9. 10.1186/s42252-025-00068-8.

[33] F. Dai, Q. Zhuang, G. Huang, H. Deng, and X. Zhang. (2023). "Infrared Spectrum Characteristics and Quantification of OH Groups in Coal". *ACS Omega.* **8** (19): 17064-17076. 10.1021/acsomega.3c01336.

[34] X. Guo, L. Liu, J. Wu, J. Fan, and Y. Wu. (2018). "Qualitatively and Quantitatively Characterizing Water Adsorption of a Cellulose Nanofiber Film Using Micro-FTIR Spectroscopy". *RSC Advances.* **8** (8): 4214-4220. 10.1039/C7RA09894D.

[35] H. Schott. (1992). "Swelling Kinetics of Polymers". *Journal of Macromolecular Science Part B: Physics.* **31** (1): 1-9. 10.1080/00222349208215453.

[36] P. L. Ritger and N. A. Peppas. (1987). "A Simple Equation for Description of Solute Release I: Fickian and Non-Fickian Release from Non-Swellable Devices in the Form of Slabs, Spheres, Cylinders or Discs". *Journal of Controlled Release.* **5** (1): 23-36. 10.1016/0168-3659(87)90034-4.

[37] F. Ganji, F. S. Vasheghani, and F. E. Vasheghani. (2010). "Theoretical Description of Hydrogel Swelling: A Review". *Iranian Polymer Journal.* **19** (5): 375-398.

[38] N. A. Peppas and J. J. Sahlin. (1989). "A Simple Equation for the Description of Solute Release III: Coupling of Diffusion and Relaxation". *International Journal of Pharmaceutics.* **57** (2): 169-172. 10.1016/0378-5173(89)90306-2.

[39] P. J. Flory and J. Rehner. (1943). "Statistical Mechanics of Cross-Linked Polymer Networks II: Swelling". *The Journal of Chemical Physics.* **11** (11): 521-526. 10.1063/1.1723792.

[40] I. Dellatolas, M. Bantawa, B. Damerau, M. Guo, T. Divoux, E. Del Gado, and I. Bischofberger. (2023). "Local Mechanism Governs Global Reinforcement of Nanofiller-Hydrogel Composites". *ACS Nano.* **17** (21): 20939-20948. 10.1021/acsnano.3c00716.

[41] W. X. Waresindo, H. R. Luthfianti, D. Edikresnha, T. Suciati, F. A. Noor, and K. Khairurrijal. (2021). "A Freeze-Thaw PVA Hydrogel Loaded with Guava Leaf Extract: Physical and Antibacterial Properties". *RSC Advances.* **11** (48): 30156-30171. 10.1039/D1RA04092H.

[42] H. R. Luthfianti, W. X. Waresindo, D. Edikresnha, A. Chahyadi, T. Suciati, F. A. Noor, and K. Khairurrijal. (2023). "Physicochemical Characteristics and Antibacterial Activities of Freeze-Thawed Polyvinyl Alcohol/Andrographolide Hydrogels". *ACS Omega.* **8** (3): 2915-2923. 10.1021/acsomega.2c05110.

[43] E. M. Ahmed. (2015). "Hydrogel: Preparation, Characterization, and Applications: A Review". *Journal of Advanced Research.* **6** (2): 105-121. 10.1016/j.jare.2013.07.006.

[44] E. Caló and V. V. Khutoryanskiy. (2015). "Biomedical Applications of Hydrogels: A Review of Patents and Commercial Products". *European Polymer Journal.* **65** : 252-267. 10.1016/j.eurpolymj.2014.11.024.

[45] H. Tian, Z. Tang, X. Zhuang, X. Chen, and X. Jing. (2012). "Biodegradable Synthetic Polymers: Preparation, Functionalization and Biomedical Application". *Progress in Polymer Science.* **37** (2): 237-280. 10.1016/j.progpolymsci.2011.06.004.

[46] R. Foudazi, R. Zowada, I. Manas-Zloczower, and D. L. Feke. (2023). Porous hydrogels: Present challenges and Future opportunities. *Langmuir.* **39** (6): 2092–2111. 10.1021/acs.langmuir.2c02253.

[47] D. Cree, S. Owuamanam, and M. Soleimani. (2023). "Mechanical Properties of a Bio-Composite Produced from Two Biomaterials:

Polylactic Acid and Brown Eggshell Waste Fillers". *Waste.* **1** (3): 740-760. 10.3390/waste1030044.

[48] N. Vu, T. Dinh, T. Le, T. Vu, T. Nguyen, T. Pham, S. Koji, S. Hama, I. Kim, D. Jang, D. Kim, and A. Tran. (2022). "Eggshell Powder as Calcium Source on Growth and Yield of Groundnut (Arachis hypogaea L.)". *Plant Production Science.* **25** (4): 413-420. 10.1080/1343943X.2022.2120506.

[49] F. Afnan, M. N. H. Kashem, R. Joshi, C. Simpson, and W. Li. (2024). "Growth of Romaine Lettuce in Eggshell Powder Mixed Alginate Hydrogel in an Aeroponic System for Water Conservation and Vitamin C Biofortification". *Gels.* **10** (5): 322. 10.3390/gels10050322.

[50] E. L. Krasnopeeva, G. G. Panova, and A. V. Yakimansky. (2022). "Agricultural Applications of Superabsorbent Polymer Hydrogels". *International Journal of Molecular Sciences.* **23** (23): 15134. 10.3390/ijms232315134.

[51] A. Garcia-Garcia, S. Munana-Gonzalez, S. Lanceros-Mendez, L. Ruiz-Rubio, L. P. Alvarez, and J. L. Vilas-Vilela. (2024). "Biodegradable Natural Hydrogels for Tissue Engineering, Controlled Release, and Soil Remediation". *Polymers.* **16** (18): 2599. 10.3390/polym16182599.

[52] A. G. Bengough, B. M. McKenzie, P. D. Hallett, and T. A. Valentine. (2011). "Root Elongation, Water Stress, and Mechanical Impedance: A Review of Limiting Stresses and Beneficial Root Tip Traits". *Journal of Experimental Botany.* **62** (1): 59-68. 10.1093/jxb/erq350.

[53] S. R. Tracy, C. R. Black, J. A. Roberts, C. Sturrock, S. Mairhofer, J. Craigon, and S. J. Mooney. (2012). "Quantifying the Impact of Soil Compaction on Root System Architecture in Tomato (Solanum lycopersicum) by X-Ray Micro-Computed Tomography". *Annals of Botany.* **110** (2): 511-519. 10.1093/aob/mcs031.

[54] P. Hinsinger. (2001). "Bioavailability of Soil Inorganic Phosphorus in the Rhizosphere as Affected by Root-Induced Chemical Changes: A Review". *Plant and Soil.* **237** (2): 173-195. 10.1023/A:1013351617532.

[55] D. L. Jones, A. Hodge, and Y. Kuzyakov. (2004). "Plant and Mycorrhizal Regulation of Rhizodeposition". *New Phytologist.* **163** (3): 459-480. 10.1111/j.1469-8137.2004.01130.x.

[56] P. J. White and M. R. Broadley. (2003). "Calcium in Plants". *Annals of Botany.* **92** (4): 487-511. 10.1093/aob/mcg164.

[57] P. Vedovello, L. V. Sanches, G. Da Silva Teodoro, V. F. Majaron, R. Bortoletto-Santos, C. Ribeiro, and F. F. Putti. (2024). "An Overview of Polymeric Hydrogel Applications for Sustainable Agriculture". *Agriculture.* **14** (6): 840. 10.3390/agriculture14060840.

[58] K. Ali, Z. Asad, G. H. D. Agbna, A. Saud, A. Khan, and S. J. Zaidi. (2024). "Progress and Innovations in Hydrogels for Sustainable Agriculture". *Agronomy.* **14** (12): 2815. 10.3390/agronomy14122815.

[59] T. Jing, J. Li, Y. He, A. Shankar, A. Saxena, A. Tiwari, K. C. Maturi, M. K. Solanki, V. Singh, M. A. Eissa, Z. Ding, J. Xie, and M. K. Awasthi. (2024). "Role of Calcium Nutrition in Plant Physiology: Advances in Research and Insights into Acidic Soil Conditions - A Comprehensive Review". *Plant Physiology and Biochemistry.* **210** : 108602. 10.1016/j.plaphy.2024.108602.

[60] H. Wang, G. Qu, X. Liu, M. He, C. Yin, and R. Xu. (2025). "Hydrogel Materials in Agriculture: A Review". *Journal of Environmental Chemical Engineering.* **13** (3): 116385. 10.1016/j.jece.2025.116385.

[61] C. Qin, H. Wang, Y. Zhao, Y. Qi, N. Wu, S. Zhang, and W. Xu. (2024). "Recent Advances of Hydrogel in Agriculture: Synthesis, Mechanism, Properties and Applications". *European Polymer Journal.* **219** : 113376. 10.1016/j.eurpolymj.2024.113376.

[62] L. Deng, H. H. Ngo, and W. Guo. (2022). “Algae-based agarose biomaterials: Production and applications”. *Elsevier eBooks*. 81–104. 10.1016/b978-0-323-96142-4.00005-1.